Plant Molecular Biology (2024) 114:4
https://doi.org/10.1007/s11103-023-01408-7

Identification and characterization of GLYCEROLIPASE A1 for wound-triggered JA biosynthesis in *Nicotiana benthamiana* leaves

Rebekah E. Holtsclaw[1,2] · Sakil Mahmud[1] · Abraham J. Koo[1]

Received: 28 July 2023 / Accepted: 3 December 2023 / Published online: 16 January 2024

Abstract

Although many important discoveries have been made regarding the jasmonate signaling pathway, how jasmonate biosynthesis is initiated is still a major unanswered question in the field. Previous evidences suggest that jasmonate biosynthesis is limited by the availability of fatty acid precursor, such as α-linolenic acid (α-LA). This indicates that the lipase responsible for releasing α-LA in the chloroplast, where early steps of jasmonate biosynthesis take place, is the key initial step in the jasmonate biosynthetic pathway. *Nicotiana benthamiana* glycerol lipase A1 (NbGLA1) is homologous to *N. attenuata* GLA1 (NaGLA1) which has been reported to be a major lipase in leaves for jasmonate biosynthesis. NbGLA1 was studied for its potential usefulness in a species that is more common in laboratories. Virus-induced gene silencing of both NbGLA1 and NbGLA2, another homolog, resulted in more than 80% reduction in jasmonic acid (JA) biosynthesis in wounded leaves. Overexpression of NbGLA1 utilizing an inducible vector system failed to increase JA, indicating that transcriptional induction of *NbGLA1* is insufficient to trigger JA biosynthesis. However, co-treatment with wounding in addition to *NbGLA1* induction increased JA accumulation several fold higher than the gene expression or wounding alone, indicating an enhancement of the enzyme activity by wounding. Domain-deletion of a 126-bp C-terminal region hypothesized to have regulatory roles increased NbGLA1-induced JA level. Together, the data show NbGLA1 to be a major lipase for wound-induced JA biosynthesis in *N. benthamiana* leaves and demonstrate the use of inducible promoter-driven construct of NbGLA1 in conjunction with its transient expression in *N. benthamiana* as a useful system to study its protein function.

Keywords *Nicotiana Benthamiana* · Wound · Jasmonate · Lipase · Glycerolipase A1 · NbGLA1 · Phospholipase A1 · PLA1 · Jasmonic acid · JA · jasmonoyl-L-isoleucine · JA-Ile

Introduction

Jasmonates are a class of hormones derived from fatty acids (FAs) that are responsible for defending plants against various abiotic and biotic stressors (Wasternack and Hause 2013). The current model of wound-activated jasmonate signaling places the biosynthesis of jasmonates upstream of the wound-induced gene expression and physiological responses (Howe et al. 2018), but how the biosynthetic pathway is triggered is still an ongoing area of research (Koo and Howe 2009; Mielke et al. 2021).

All biosynthetic enzymes involved in the jasmonate pathway have been identified and localized to either the chloroplast, peroxisome, or cytosol (Koo 2018; Vick and Zimmerman 1983; Schaller and Stintzi 2009; Wasternack and Feussner 2018). The main precursor is an 18-carbon FA with three double bonds at the carbon 9, 12, and 15 positions, designated as 18:3 $\Delta^{9,12,15}$, also known as a-linolenic acid (α-LA), which is hydrolyzed from membrane glycerol lipids. Upon release, α-LA is oxygenated and cyclized to form a cyclopentanone intermediate, 12-oxo-phytodienoic acid (OPDA). This is the last intermediate produced in the chloroplast. OPDA is then transferred to the peroxisome and further metabolized by losing six carbons via b-oxidation steps to yield 12-carbon, jasmonic acid (JA). JA is then exported to the cytosol and conjugated to the amino acid

✉ Abraham J. Koo
kooaj@missouri.edu

[1] Department of Biochemistry, University of Missouri, 65211 Columbia, MO, USA

[2] Present address: Rubi Laboratories, 94577 San Leandro, CA, USA

isoleucine to form jasmonoyl-L-isoleucine (JA-Ile) (Staswick and Tiryaki 2004), which is a bioactive form of jasmonates (Fonseca et al. 2009; Katsir et al. 2008a).

There are several lines of evidence suggesting that JA biosynthesis is limited by substrate availability (Miersch and Wasternack 2000; Wasternack 2007; Koo et al. 2009). One observation supporting this is that feeding plants or isolated intact chloroplasts with exogenous α-LA leads to JA or OPDA accumulation, respectively, without additional elicitation (Kimberlin et al. 2022; Vick and Zimmerman 1983; Christeller and Galis 2014). This indicates that plant cells have all the necessary enzymes to convert α-LA to JA or OPDA and that no further activation is required for those enzymes to complete JA biosynthesis. Therefore, the step that generates the α-LA substrate is the key limiting step for JA biosynthesis.

The α-LA substrate is generated by A-type phospholipases (PLAs) (Ryu 2004; Kelly and Feussner 2016; Wang 2001). In Arabidopsis, there are seven genes referred to as plastidial *DAD1-like PLA1s* (Rudus et al. 2014), named after one of its members, *DEFECTIVE IN ANTHER DEHISCENCE 1* (*DAD1*), which is known to catalyze JA biosynthesis during flower development (Ishiguro et al. 2001). The *DAD1* mRNA transcript is also highly induced among plastidial *PLA1s* upon wounding in leaves, and its ectopic expression in Arabidopsis leaves leads to the production of JA (Kimberlin et al. 2022; Rudus et al. 2014), suggesting its major role in JA biosynthesis in leaves. However, the *dad1* mutant does not display significant reduction in overall JA level in wounded leaves, indicating a contribution by other PLA1s in this process (Ellinger et al. 2010; Hyun et al. 2008; Wang et al. 2018; Yang et al. 2007). Recently, one of these members, DALL2 (AtPLA1-Ig3), was reported to function in the primary vasculature to produce OPDA and OPDA-containing galactolipids, and plays role in wound-induced systemic JA production in the leaves distal to wound sites (Morin et al. 2023). In contrast to the gene redundancy issues of *Arabidopsis* PLA1s, a dominant lipase involved in wound-induced JA biosynthesis called glycerolipase A1 (NaGLA1) was reported in *Nicotiana attenuata* (Kallenbach et al. 2010). Knocking down NaGLA1 expression in *N. attenuata* resulted in greater than an 80% reduction in wound-induced JA levels.

Considering the significance of NaGLA1 as a pivotal lipase in wound-induced JA production within *N. attenuata* species, which exhibit fewer challenges related to gene redundancy compared to Arabidopsis, and to facilitate convenient laboratory experimentation, we have opted to investigate GLAs in *N. benthamiana* as a more feasible alternative to the wild *N. attenuata* species. Furthermore, the availability of the public genome sequence for *N. benthamiana* (Bombarely et al. 2012) further supports its suitability as a research model. Our research initially focuses on examining the time course of wound- and exogenous α-LA-dependent jasmonate synthesis in *N. benthamiana* leaves. We then identify and characterize the functional *N. benthamiana* homolog of NaGLA1 using virus-induced gene silencing (VIGS) (Dommes et al. 2019). To evaluate the impact of gene expression and wounding on NbGLA1 enzyme activity for JA biosynthesis, we employ a dexamethasone (dex)-inducible system (Aoyama and Chua 1997). Sequence analysis and computational modeling were applied to identify domains hypothesized to have regulatory roles. Structure-function analysis was then carried out on one of those domains at the C-terminus using a deletion construct. Overall, our study identified NbGLA1 as a major lipase involved in the regulation of JA biosynthesis in *N. benthamiana* and furthermore, we propose that the post-transcriptional regulation represents a conserved mechanism in both *Arabidopsis* and *Nicotiana* species during the initiation process to trigger JA biosynthesis upon leaf wounding.

Materials and methods

Chemicals and biological materials

(±)-Jasmonic acid (JA), coronatine (COR), α-LA ((9*Z*,12*Z*,15*Z*)-octadeca-9,12,15-trienoic acid), dexamethasone (dex), and cycloheximide (CHX) were purchased from MilliporeSigma (Burlington, MA). Dihydro-JA, jasmonoyl-L-isoleucine (JA-Ile), [$^{13}C_6$]-JA-Ile, 12-oxophytodienoic acid (OPDA), and [$^{2}H_5$]-OPDA were obtained as previously described (Koo et al. 2009). Wild-type (WT) *Nicotiana benthamiana* plants were grown at 22 °C under a 16-h-light photoperiod with a light intensity of 130–150 μE m^{-2} s^{-1}. The *Agrobacterium tumefaciens* strain C58C1 was used for all dex-inducible vector expression studies, and the strain GV3101 was used for VIGS experiments.

Dex-inducible system and agrobacterium infiltration

Several versions of *NbGLA1* constructs, including full-length (*Pdex:NbGLA1*), C-terminal truncated (*Pdex:NbGLA1-D*), or active site-mutated (*Pdex:NbGLA1^{mut}*), were cloned into a glucocorticoid-inducible vector system (*Pdex*) (Aoyama and Chua 1997) utilizing *Xho*I and/or *Spe*I as restriction enzyme sites. The primers used to clone these constructs are listed in Supplemental Table S1. The inserts were PCR-amplified using a Phusion High-Fidelity Polymerase (New England Biolabs, Ipswich, MA) and cloned into pGEM-T Easy vector system (Promega, Madison, WI). After sequence verification, each insert was subcloned into

the *Pdex* vector. Site-directed mutagenesis was performed using the Q5 Site-Directed Mutagenesis Kit (New England BioLabs, Ipswich, MA) according to the manufacturer's instructions. Mutagenesis reactions were performed on *NbGLA1* in pGEM-Teasy vector as a template, resulting in the substitution of the lipase consensus motif GSHLG to AAAAA (*Pdex:NbGLA1*^{mut}).

The above constructs were then transformed into the C58C1 strain of *Agrobacterium tumefaciens*. Transient expression in *N. benthamiana* leaves was carried out using syringe infiltration of *Agrobacteria* carrying the transgene constructs, as previously described (Koo et al. 2009; Ryu et al. 2004). Bacterial cultures ($OD_{600} = 0.2$) were resuspended in infiltration buffer (10 mM MES, pH 5.6, 10 mM $MgCl_2$) and supplemented with 150 µg/mL acetosyringone immediately prior to use. The 2nd and 3rd youngest leaves of 4-week old *N. benthamiana* leaves were infiltrated on both halves of each leaf (either side with the midvein in the middle). Needleless syringes were used to infiltrate the abaxial side of the leaf. The agroinfiltrated plants were kept in the dark for 16 h, then moved to light for the next two days to allow transfection. To induce transgene expression, 30 µM dex (0.01% (v/v) DMSO and 0.01% (v/v) Triton x-100) was sprayed to saturate the leaf surface for 6 h prior to other treatments, such as wounding, unless stated otherwise in the results. COR pre-treatment was done by spraying 5 µM COR solution on the surface of leaves for 30 or 60 min. The α-LA feeding experiment was conducted by incubating *N. benthamiana* leaf discs (11 mm diameter) in liquid Murashige & Skoog (MS) media containing 100 µM α-LA. Discs were punched out from leaves and initially floated in MS media for 1 h without α-LA until JA levels stabilized to background levels. The media was then replaced with that media w/ or w/o 100 µM α-LA (in < 0.01% DMSO) and further incubated for durations indicated in figures when leaf discs were recovered for hormone extraction.

The wounding treatment described in Fig. 1 involved creating 3–4 wounds across the leaves of 3-week-old *N. benthamina* plants perpendicular to the midvein using a pair of hemostats with serrated tips. The wounds were made in the direction from the tip to the petiole of the leaf. Whole leaf was processed for RNA or hormone extraction. For the wounding treatment used in conjunction with Agrobacterium infiltration, a similar approach was followed except that the leaf samples were collected using an 11 mm diameter hole punch, with one line of wounding marks running across each punched-out disc. These leaf discs were then placed in a tube with metal beads and quickly frozen with liquid nitrogen. A tissue homogenizer (TissueLyserII, Qiagen) was used to pulverize samples into a fine powder for hormone and RNA extractions.

Virus-induced gene silencing (VIGS)

The pTRV1 (CD3-1039) and pTRV2 (CD3-1040) vectors were purchased from the Arabidopsis Biological Resource Center (Ohio State University) (Burch-Smith et al. 2006). Utilizing the VIGS Tool available at Sol Genomics Network (solgenomics.net), an overlapping fragment of 185 bp in the *NbGLA1* and *NbGLA2* genes was PCR-amplified with primers shown in supplemental Table S2 and was inserted into the pTRV2 vector using *EcoR*I and *BamH*I restriction sites. The resulting pTRV2 and pTRV1 plasmids were each transformed into *Agrobacterium* (GV3101 strain). Half-and-half volume mixture of each bacterial clone was co-infiltrated into *N. benthamiana* leaves as described previously (Ratcliff et al. 2001). Control infection involved TRV1 vector infiltrated together with an empty TRV2 vector. Tissue samples were processed 3 weeks post infection.

Quantification of JA derivatives

JA metabolites were extracted into a 70% methanolic solvent (with 0.5% (v/v) acetic acid in water) containing dihydro JA (dhJA) and [$^2H_5$]-OPDA as internal standards. An ultra-performance liquid chromatography (ACUITY H-class, Waters, MA, USA) coupled to a triple quadrupole tandem mass spectrometer (MS/MS) (Xevo T-QS, Waters, MA, USA) was used to analyze the extracted metabolites, according to previously established methods (Koo et al. 2014). Seven microliters of samples were injected and separated on a C18 column (2.7 µm, 2.1 × 50 mm; Ascentis Express, Millipore Sigma, MO, USA) which was maintained at 40 °C. A 3-min gradient inlet program pumped methanol (mobile A) and 0.1% aqueous formic acid (mobile B) as a mobile phase at a 0.4 ml min^{-1} flow rate. Characteristic MS/MS transitions of *m/z* 209 > 59 (JA), 211 > 59 (dhJA), 291 > 165 (OPDA), and 296 > 170 ([$^2H_5$]-OPDA) were used to analyze each compound in a Multiple Reaction Monitoring mode. The limit of quantification for the analyte standards mixed with *N. benthamiana* leaf extract as matrix was 1 nM for JA and OPDA, and 0.1 nM for JA-Ile. Data acquisition and analysis were carried out using MassLynx 4.1 and TargetLynx software (Waters, MA, USA). The quantification was based on the analyte comparisons to calibration curves generated using known amounts of JA and OPDA references relative to quantities of their respective internal standards.

RNA analysis

TRIzol reagent (Thermo Fisher Scientific, MA, USA) was used to isolate total RNA from 15 to 20 mg tissues following the manufacturer's instruction. One microgram of

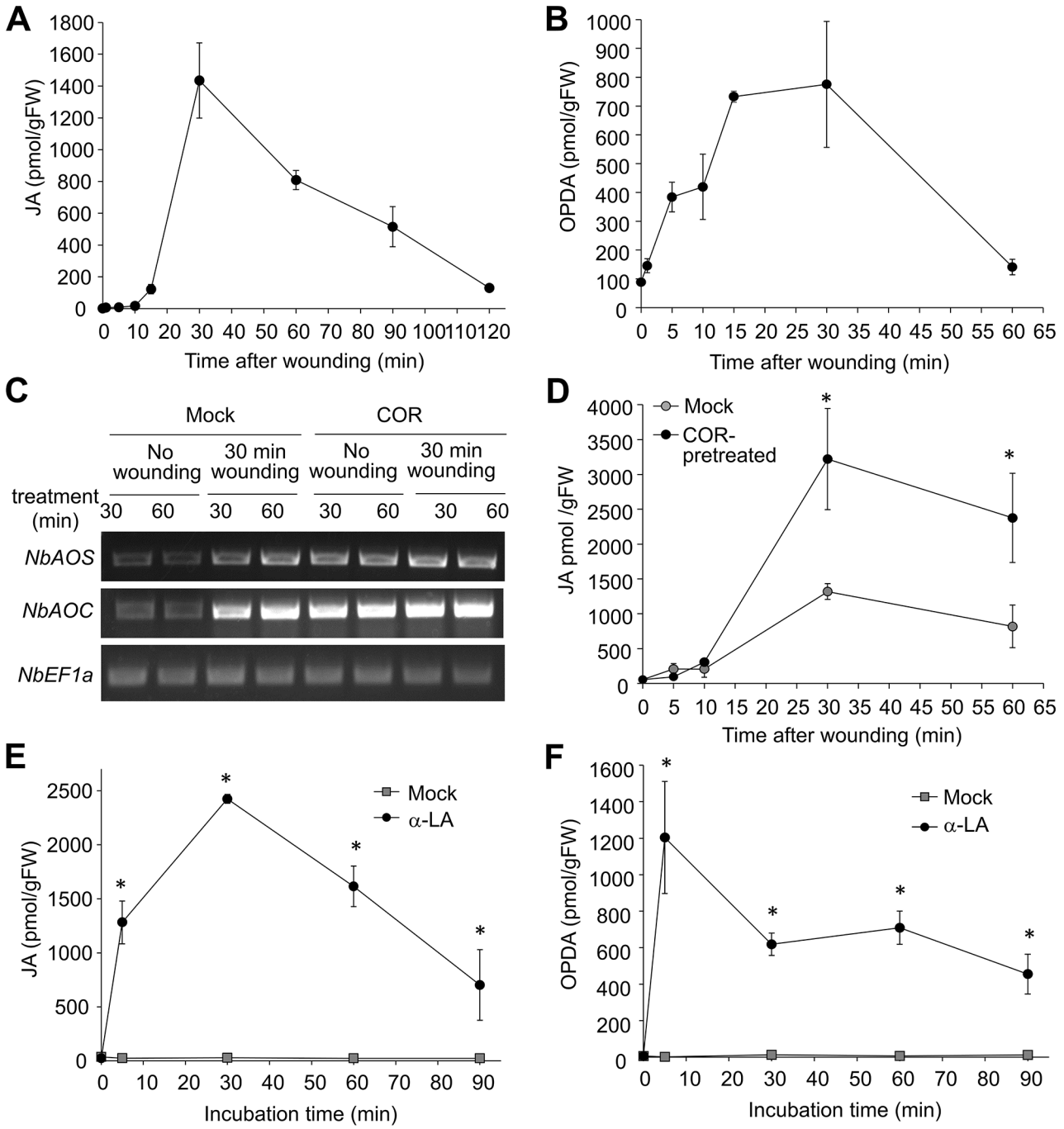

Fig. 1 Time course shows an initial lag in JA biosynthesis but no lag in OPDA production in wounded *N. benthamiana* leaves. (**A**-**B**) Levels of JA (**A**) and OPDA (**B**) in wounded *N. benthamiana* leaves (3-week-old). (**C**) Agarose gel image displaying the results of RT-PCR, indicating the induction of JA marker genes *NbAOS* (Niben101Scf10535g00001.1) and *NbAOC* (Niben101Scf13816g00005.1) in wounded leaves (30 min) and unwounded leaves with or without (Mock) 5 µM coronatine (COR) pre-treatment for 30 or 60 min. *NbEF1a* (01Scf08618g01012.1) was amplified as an internal reference. (**D**) Time course of JA levels in wounded leaves pre-treated with 5 µM COR or Mock (0.01% (v/v) ethanol in water) for 30 min. (**E**-**F**) Levels of JA and OPDA in leaves incubated with Mock (0.01% (v/v) DMSO in water) or α-LA (100 µM). Error bars indicate the standard deviation of 3–4 biological replicates. Asterisks indicate statistical significance ($P < 0.01$, student *t*-test)

total RNA was reverse transcribed using oligo $(dT)_{20}$ primers and iScript Reverse Transcription Supermix (BioRad, Hercules, CA, USA). An aliquot of the resulting cDNA was used as a template for PCR using Bioline BioMix Red (Meridian Bioscience inc., London, UK). qPCR was performed using iTaq SYBR™ Green Supermix (BioRad) in a CFX96 Touch™ real-time PCR detection system (BioRad). *NbAOS* (*Niben101Scf10535g00001.1*), *NbAOC* (*Niben101Scf13816g00005.1*), and *NbEF1a* (*Niben101Scf08653g00001.1*) were the sequence homologs to the previously described genes in *N. attenuata* (Kallenbach et al. 2010). *NbEF1a* was used as an internal reference gene. Primers used can be found in Supplemental Table S1.

Sequence analysis and structural modeling

Sequences were obtained from the Sol Genomics Network (solgenomics.net) and Queenslad University of Technology Consortium (https://benthgenome.qut.edu.au/). Sequence alignment was carried out using the combined multiple aligners (M-Coffee) from the T-Coffee (http://tcoffee.crg.cat/apps/tcoffee/index.html) (Di Tommaso et al. 2011) with the standard settings. The phylogeny was constructed using the maximum likelihood method through MegaX software (https://www.megasoftware.net/) (Kumar et al. 2018). The resulting tree file was uploaded to the Interactive Tree of Life (iTOL) webserver (https://itol.embl.de/) for formatting (Letunic and Bork 2021). A consensus tree was created based on 100 bootstrap replications. Subcellular localization was predicted using TargetP2.0 (https://services.healthtech.dtu.dk/services/TargetP-2.0/) (Almagro Armenteros et al. 2019). Two approaches were used for structure modeling. First, a homology-based modeling approach was employed using ModWeb (https://modbase.compbio.ucsf.edu/modweb/) (Pieper et al. 2009). The second approach utilized Iterative Threading ASSEmbly Refinement (I-TASSER), which first identifies templates from the Protein Data Bank (PDB) through a multiple threading approach and assembles full-length atomic models (Yang et al. 2015). Pictures of the models were generated using MacPymol 2.0 (Schrödinger Inc.). Phosphorylation site predictions were made using MusiteDeep (https://www.musite.net) (Wang et al. 2020).

Results

OPDA increases within minutes of wounding *N. benthamiana* leaves

Basal levels of jasmonates in leaves are known to be low, detectable only by sensitive modern mass spectrometers (Glauser et al. 2009). Tissue damage caused by insect herbivory or deliberate mechanical wounding elicits an immediate and linear increase of JA in *Arabidopsis* leaves (Glauser et al. 2008; Chung et al. 2008). To determine whether this is conserved in our model system *N. benthamiana*, a similar time course experiment was carried out. Four-week-old *N. benthamiana* leaves were crushed perpendicularly to the midvein using a pair of hemostats, and tissue samples were analyzed for OPDA and JA contents. In contrast to the findings reported in *Arabidopsis* (Chung et al. 2008; Glauser et al. 2008), there was a clear lag period of about 10–15 min before JA levels started to steeply rise, peaking around 30 min (Fig. 1A). However, the OPDA levels increased quickly within few minutes without any perceivable delay (Fig. 1B). These results indicate that the initiation of wound-triggered OPDA biosynthesis in *N. benthamiana* follows a similar trend to *Arabidopsis*. However, there seem to be additional step(s) downstream of OPDA synthesis that limit the early rise in JA levels in *N. benthamiana*.

To investigate whether 'priming' the JA biosynthetic pathway by pre-inducing the expression of JA biosynthetic genes would alleviate the initial lag of JA biosynthesis, plants were sprayed with coronatine (COR) (50 µM) 30 or 60 min prior to wounding. COR, a structural mimic of JA-Ile, is known to induce most genes in the JA biosynthetic pathway without the need for wounding (Katsir et al. 2008b; Attaran et al. 2014). RNA analysis confirmed the effectiveness of the COR treatment (Fig. 1C). However, there was no change to the 10-min lag for wound-induced JA accumulation (Fig. 1D), suggesting that the lag is unlikely to be due to a delay in the gene expression of JA biosynthetic enzymes. It is noted that the COR pre-treatment alone did not trigger JA biosynthesis (as seen in 0 min data point in the Fig. 1D), consistent with previous reports using COR (Koo et al. 2009; Kimberlin et al. 2022) or its structural variants (Koch et al. 1999; Miersch and Wasternack 2000; Pluskota et al. 2007; Scholz et al. 2015). However, the COR pre-treatment did help to elevate the wound-induced level of JA content (Fig. 1D), which differs from observations in Arabidopsis, where no enhancement in wound-induced JA was observed (Kimberlin et al. 2022), indicating variations in metabolic regulation between the two species.

We then examined the conversion of exogenously treated α-LA to OPDA and JA without wounding (Fig. 1E and F). Similar to previous findings in Arabidopsis and rice (Vick and Zimmerman 1983; Farmer and Ryan 1992; McConn and Browse 1996; Christeller and Galis 2014; Kimberlin et al. 2022), α-LA was converted to OPDA and JA, indicating that the system is not limited with respect to the biosynthetic capacity downstream of α-LA.

NbGLA1 and *NbGLA2* of *N. benthamiana* represent the most closely related homologs to *NaGLA1* of *N. attenuata*

In 2010, NaGLA1 was reported as the primary lipase responsible for the majority (75–80%) of JA production in wounded *N. attenuata* leaves (Kallenbach et al. 2010). We conducted a search for sequences in *N. benthamiana* using data from both Sol Genomics Network (https://solgenomics.net/) and Queensland University of Technology Consortium (https://benthgenome.qut.edu.au/). BLAST query of Sol Genomics Network (genome release, v1.0.1) using the full length NaGLA1 amino acid sequence (GenBank: OIS99680.1) resulted with an *N. benthamiana* sequence (Niben101Scf00428g11016.1) with 96% identity to NaGLA1, which we designated as NbGLA1 (Fig. 2). Three other sequences, Niben101Scf06078g02033.1 (NbGLA2), Niben101Scf09317g01012.1 (NbGLA3), and Niben101Scf05956g01009.1 (NbGLA4) were also found, displaying lower sequence identities of 88%, 72%, and 70%, respectively, to NaGLA1. To visualize the relationships between PLA1-like sequences in *N. benthamiana* and the

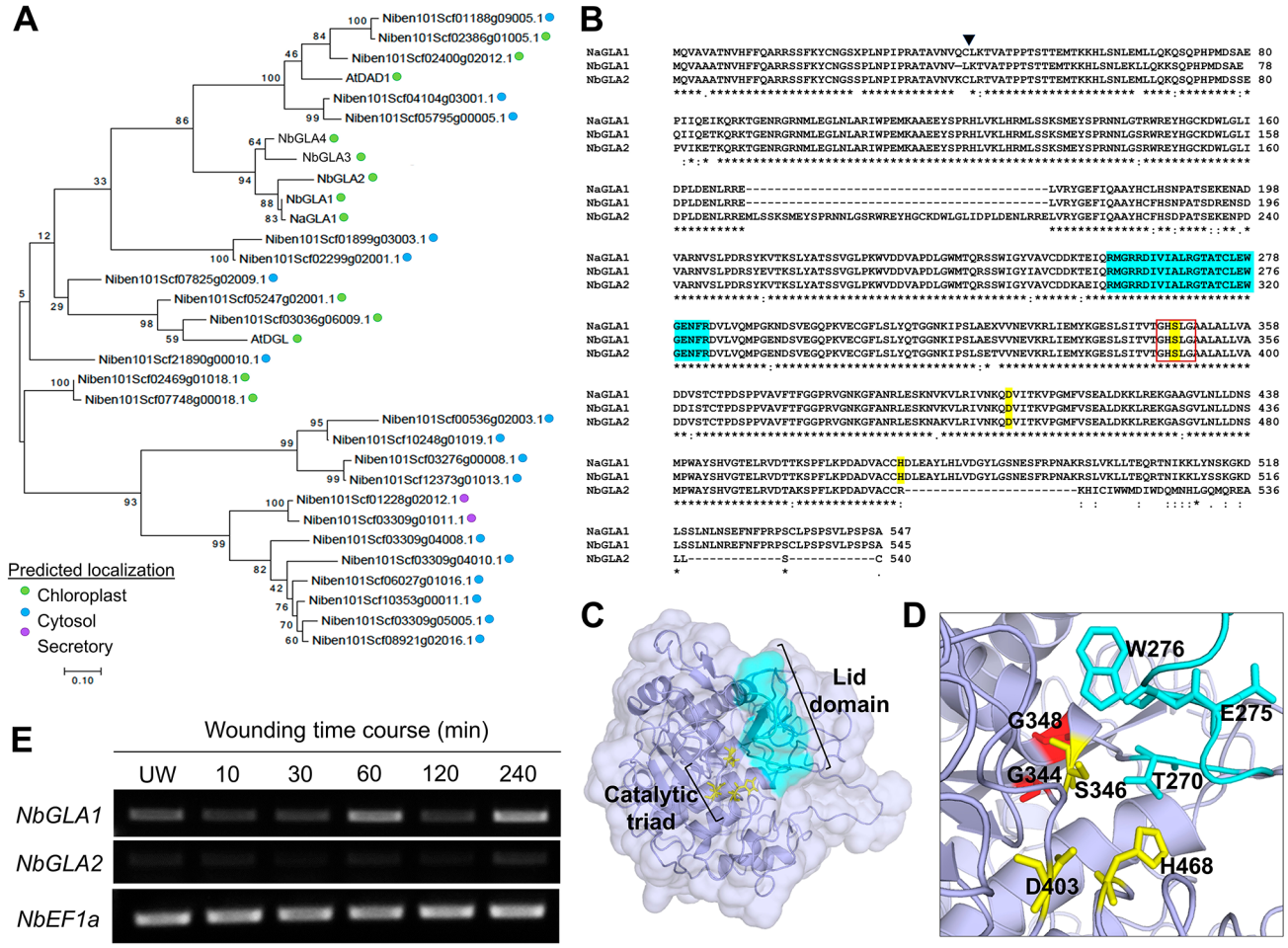

Fig. 2 *NbGLA1* and *NbGLA2* are the closest homologs to *NaGLA1*. (**A**) Phylogenetic relationships among PLA1 protein sequences from *N. benthamiana* and selected sequences from *A. thaliana* and *N. attenuata*. Sequences were obtained from TAIR10 (*Arabidopsis*), SolGenomics (*N. benthamiana*), and NCBI (*N. attenuata*). The tree was constructed using the maximum likelihood method in MEGAX, and the resulting tree file was visualized with iTOL. Three reference PLA1s from *Arabidopsis* (AtDAD1, AtDGL) and *N. attenuata* (NaGLA1) are shown. A consensus tree, following 100 bootstrap replications, is presented with branch lengths indicating the number of sequence differences (scale = 0.1 or 10% changes). Colored circles indicate subcellular localization predictions using TargetP2.0. (**B**) Alignment of NaGLA1, NbGLA1, and NbGLA2 protein sequences. The alignment was performed using T-coffee. The predicted chloroplast transit peptide cleavage site based on TargetP2.0 prediction is marked with an inverted triangle. The putative catalytic triad is highlighted in yellow, the lid domain in cyan, and the nucleophilic elbow is boxed in red. (**C**-**D**) Modeled structure of NbGLA1 (without transit peptide) using I-TASSER. (**C**) The overall structure of NbGLA1 with its exterior surface. (**D**) A close-up view of the active site with the catalytic triad highlighted in yellow (S346, D403, H468), the two glycine residues in the GxSXG motif in red (G344, G348), and three of the five conserved residues from the lid domain in cyan (T270, E275, W276). (**E**) Wounding time course of *NbGLA1* and *NbGLA2* transcripts using RT-PCR in leaves of 3-week-old *N. benthamiana*. Wounding was administered by crushing leaves three times across the midvein with a hemostat. *NbEF1a* was amplified as an internal reference

previously reported PLA1s in *N. attenuata* (NaGLA1) and *Arabidopsis* (AtDAD1 and AtDGL), an unrooted evolutionary tree was built using the maximum likelihood algorithm and 100 bootstraps (MegaX and iTOL) (Fig. 2A). The tree included 29 PLA1-like sequences from *N. benthamiana*, obtained through a blast search using 12 *Arabidopsis* PLA1s (Ryu 2004) (Supplemental Table S2) (Full tree including all twelve DAD1-like PLA1s from Arabidopsis is shown in Supplemental Fig. S1). Among them, 11 were predicted by TargetP2.0 to localize to the plastid, clustering together with the previously known plastidial lipases (Rudus et al. 2014) involved in JA biosynthesis from *Arabidopsis* (e.g., AtDAD1) (Ishiguro et al. 2001)d *attenuata* (NaGLA1 (Kallenbach et al. 2010). Four NbGLAs formed a distinct clade with NaGLA1, and among those four, NbGLA1 and NbGLA2 clustered most closely with NaGLA1.

NbGLA1, the closest sequence to NaGLA1, has a predicted plastid transit peptide (TargetP2.0) ending at L41, a lid domain (R257-R281), and a consensus GxSxG motif that includes S346 as part of the catalytic triad, along with D403 and H468, as predicted by sequence alignment with NaGLA1 and homology modeling using I-Tasser (Yang et al. 2015) (Fig. 2B-D). The model was based on the crystal structure of Arabidopsis PLA1, AtPLA1-IIg (At4g18550, PDB ID: 2YIJ) (Fig. 2C and D). NbGLA2 closely resembled NaGLA1 and NbGLA1 in most areas, except for the insertion of a 42-amino acid stretch between E170 and L212 (Fig. 2B). NbGLA2 also diverges in sequence after C511 and had an apparent deletion in the C-terminus. This C-terminal region present in NbGLA1 but was lacking in NbGLA2 shows little sequence similarity to AtPLA1-IIg and is therefore left as an unstructured loop in our structural modeling. This region contains three serine residues that are predicted to be sites of phosphorylation, which will be discussed further.

The expression of *NbGLA1* and *NbGLA2* in wounded leaves was studied using reverse transcriptase (RT)-PCR (Fig. 2E). Between the two, *NbGLA1* exhibited higher overall expression levels, which increased at 1 h after wounding. This differs somewhat from *NaGLA1*, which was reported to slightly decrease after wounding (Kallenbach et al. 2010) but is similar to *Arabidopsis DAD1* which was strongly induced by wounding around similar time frame (Kimberlin et al. 2022).

Virus-induced gene silencing of *NbGLA1* and *NbGLA2* reduces JA accumulation

Virus-induced gene silencing (VIGS) was then employed to investigate the functional role of NbGLAs in the production of wound-induced JA. Although *NbGLA1* was determined to be the dominantly expressed member of the two, both *NbGLA1* and *NbGLA2* were targeted to increase the likelihood of observing the effects of gene silencing. To achieve this, a 185-bp segment that is shared between both sequences but not shared by any other sequences in the genome was selected using the SolGenomics VIGS tool (https://vigs.solgenomics.net/) (primers used to amplify 185-bp are shown in Supplemental Table S1). The selected segment was then cloned into a tobacco rattle virus (TRV)-based VIGS vector (Fig. 3A). As controls, *N. benthamiana* plants infected with an empty vector (EV) strain were used. The efficiency of gene-silencing was analyzed by RT-PCR in unwounded and wounded leaves of two independent *NbGLA1/2*-VIGS plants, three weeks after infiltration (Fig. 3B). Visible reductions in mRNA levels were observed for both *NbGLA1* and *NbGLA2* transcripts in the *NbGLA1/2*-VIGS plants compared to the EV controls at all time points (Fig. 3B).

Next, the levels of wound-induced JA levels in the leaves were quantified at multiple timepoints after wounding (Fig. 3C). A reduction in JA levels was observed at all timepoints, with up to a 90% decrease occurring at 30 and 60 min in the wounded *NbGLA1/2*-VIGS plants compared to the EV plants. The reduced JA levels in the VIGS plants also influenced JA-responsive marker gene, *NbAOS*, expression (Supplemental Fig. S2). *NbAOS* transcripts were significantly decreased in VIGS lines at all time points after wounding when compared to EV controls. This finding demonstrates that NbGLA1, and potentially NbGLA2, are the major lipases involved in wound-induced JA biosynthesis in *N. benthamiana* leaves as the functional orthologs of NaGLA1. It remains to be further determined which of the two plays a more dominant role. However, based on the greater sequence similarity to the published NaGLA1 and its higher expression level, NbGLA1 was chosen for subsequent studies.

Transient expression of *NbGLA1* is insufficient to induce JA biosynthesis but wounding boosts the synthesis several fold

Previous research conducted in Arabidopsis has demonstrated that the ectopic expression of a *PLA1* gene, *AtDAD1*, can result in JA accumulation (Kimberlin et al. 2022). However, it was also shown that the ability to elicit JA biosynthesis by *AtDAD1* expression was variable depending on the developmental stages of the plants (Kimberlin et al. 2022). Mature rosette leaves of plants older than 25 days accumulated JA solely through AtDAD1 expression, without the need for additional wounding. However, when the same treatment was applied to younger plants (less than 25 days old), it either did not stimulate JA biosynthesis or stimulated JA biosynthesis only to a small extent, despite the high accumulation of AtDAD1 proteins. Importantly, regardless

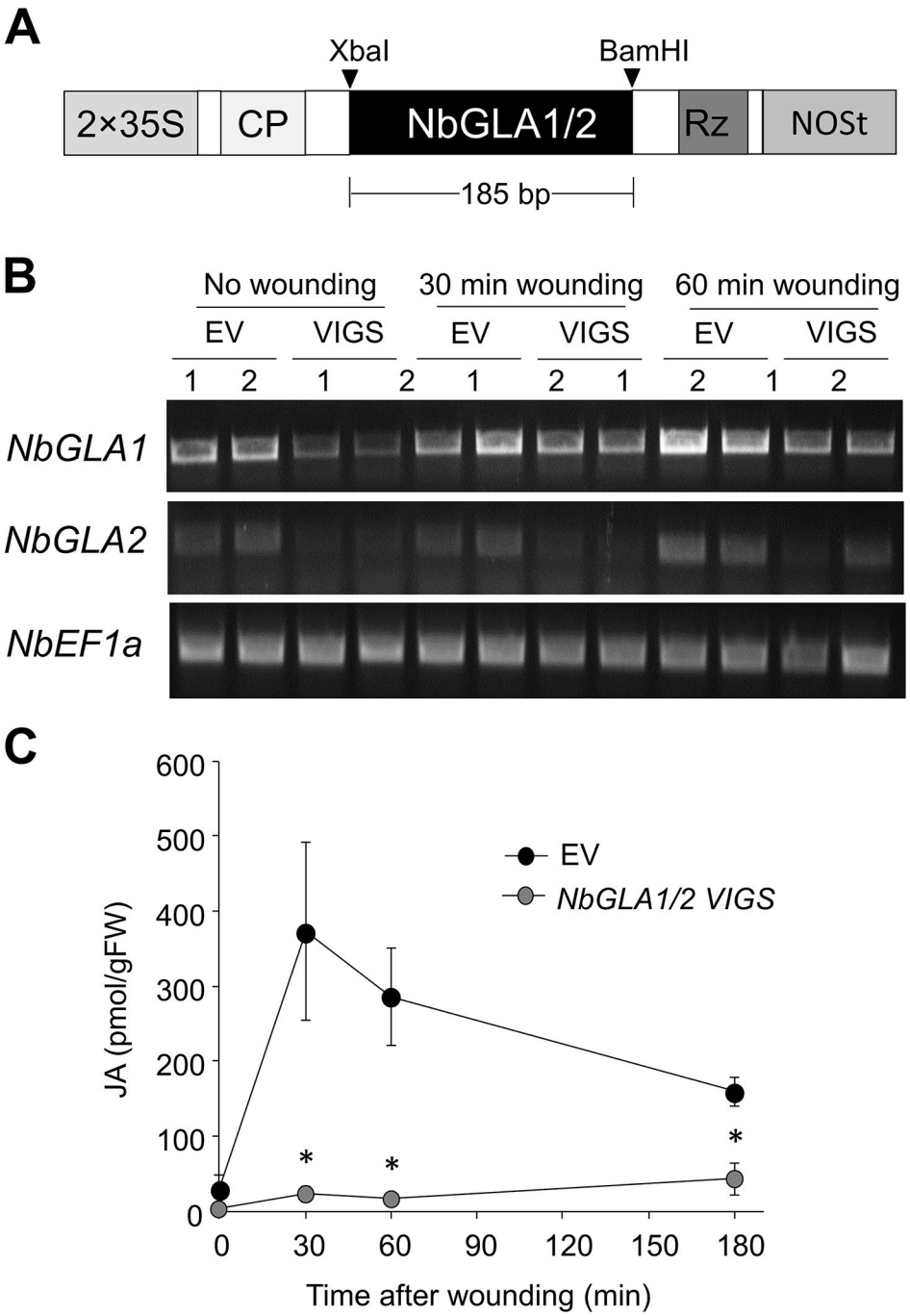

Fig. 3 Virus-induced gene silencing (VIGS) of *NbGLA1* and ***NbGLA2*** results in a significant reduction in JA content in wounded leaves. (**A**) Schematic representation of the tobacco rattle virus (TRV) based VIGS vector construct, including a 185-bp stretch of DNA sequences that are common to both *NbGLA1* and *NbGLA2*. 35 S, CaMV 35 S promoter; CP, coat protein; Rz, self-cleaving ribozyme; NOSt, nopaline synthase terminator. Not to scale. (**B**) RT-PCR analysis of *NbGLA1*, *NbGLA2*, and *NbEF1a* transcripts from wounded leaves infiltrated with either the empty vector (EV) or the NbGLA1/2 VIGS (VIGS) construct. Results from two independent VIGS plants are shown, with each replicate indicated by numbers 1 and 2. (**C**) Time course of JA accumulation after wounding *N. benthamiana* leaves expressing the EV or *NbGLA1/2* VIGS construct. The data in the graphs represent the average ± SD of four biological replicates. Asterisks indicate statistical significance ($P < 0.01$, student *t*-test)

of the plant's ages, the combination of wounding and ectopic gene expression resulted in a significant increase in JA accumulation compared to either gene expression or wounding alone (Kimberlin et al. 2022), indicating that AtDAD1 is activated by a post-transcriptional event by wounding.

A similar experiment was conducted in *N. benthamiana* with *NbGLA1*. To regulate gene expression, a dex-inducible vector system (Aoyama and Chua 1997) was utilized, allowing transient induction of *NbGLA1* expression through exogenous application of dex. The second and third youngest leaves of 4-week old *N. benthamiana* leaves were infiltrated with Agrobacteria harboring the dex-inducible *NbGLA1* construct (*Pdex:NbGLA1*). As a control, a catalytically inactive version of NbGLA1 (*Pdex:NbGLA1*^{mut}) was created by mutagenizing a highly conserved lipase domain, where the GxSxG motif was replaced with five alanine residues. This mutation resulted in the replacement of the catalytic serine (S346, Fig. 2B and D), which is essential for the

lipase activity. After two days of infiltration, the leaves were sprayed with a 30 µM dex solution. Untreated leaves (0 h) of *Pdex:NbGLA1*-infiltrated plants exhibited a similar level of *NbGLA1* transcripts compared to control leaves infiltrated with a mock solution (infiltration media without vector followed by dex treatment for indicated durations) (Supplemental Fig. S3 and Fig. 4A), indicating low background expression in the absence of the transgene. Following 4 and 6 h of dex induction, over 26-fold increase in transcripts was observed for both *NbGLA1* and *NbGLA1*^{mut}, compared to the mock treatment (Fig. 4A). JA levels were determined 6 h after dex induction and/or 30 min after wounding and/or 5.5 h dex induction followed by 30 min wounding (total 6 h dex). Without wounding, only background levels of JA was detected in the mock, *Pdex:NbGLA1* or *Pdex:NbGLA1*^{mut}, indicating that gene expression alone was insufficient to trigger JA biosynthesis (Fig. 4B). Wounding (30 min) alone increased JA levels to approximately 700 pmol/gFW in all cases as expected. However, when wounding was combined with dex, JA level rose to almost 7,000 pmol/gFW only in leaves expressing *Pdex:NbGLA1* (Fig. 4B). This dramatic increase was not observed in similarly treated mock or *Pdex:NbGLA*^{mut} leaves, suggesting that the substantial accumulation of JA relied on the strong expression of NbGLA1 and its catalytic activity. These results demonstrate that, similar to the earlier observations in Arabidopsis (Kimberlin et al. 2022), the presence of lipases alone does not trigger significant JA biosynthesis in *N. benthamiana*. Instead, an additional activation step, which can be stimulated by wounding, is required for the initiation of JA biosynthesis in both species.

Structure-function analysis of the C-terminal end of NbGLA1

Upon observing a substantial increase in JA biosynthesis upon wounding in leaves transiently over-expressing *NbGLA1*, we hypothesized that NbGLA1 might be regulated at the post-translational level. To investigate the mechanism behind this regulation, we examined the amino acid sequence and three-dimensional protein structure of NbGLA1 for features that could provide some insights for regulations. NbGLA1 (as well as NaGLA1) contains a 33-amino acid C-terminal sequence that is absent in AtDAD1 or NbGLA2 (Fig. 5A). Structural modeling (Eswar et al. 2006) of NbGLA1, using a publicly available crystal structure of AtPLA1-IIg (PBD ID:2YIJ) as a template, revealed that the 33-amino acid C-terminal domain of NbGLA1 resembled a protein-protein interaction domain involved in homodimerization in the 2Y1J structure (Fig. 5A). This region contains a relatively high proportion of serine residues (7 out of 33), some of which were predicted to be phosphorylated based on MusiteDeep predictions (Wang et al. 2020) (Fig. 5A).

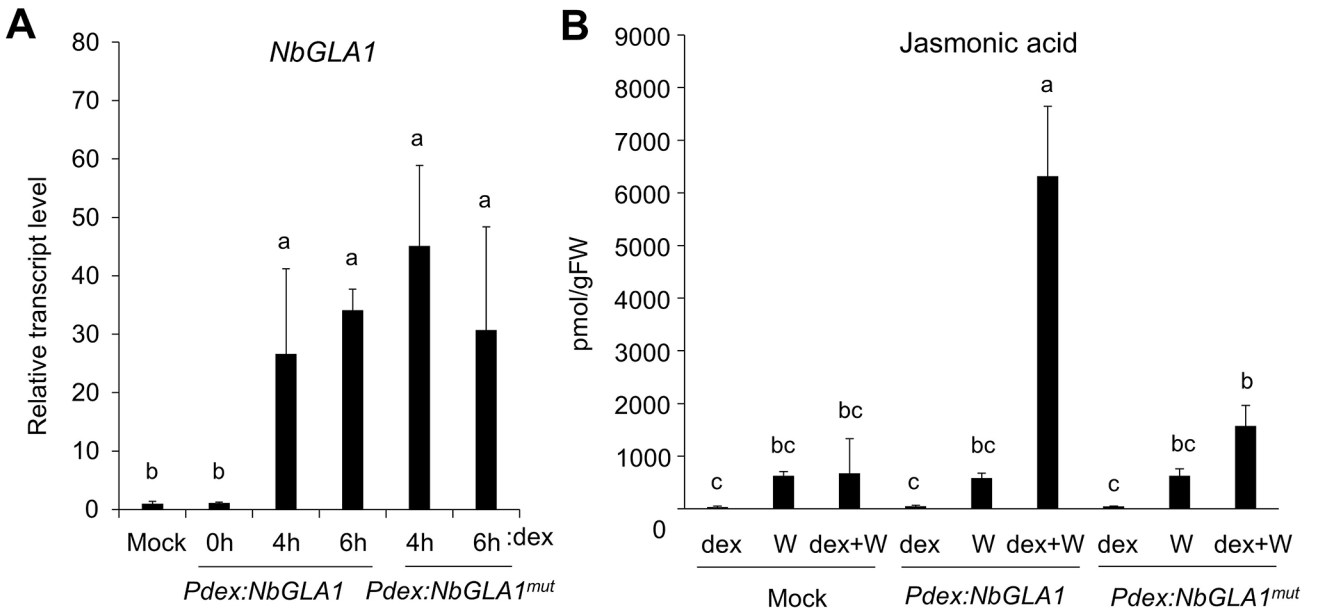

Fig. 4 JA levels in *N. benthamiana* leaves transiently expressing *NbGLA1*. (**A**-**B**) RT-qPCR (**A**) and JA measurements (**B**) in *N. benthamiana* leaves infiltrated with Agrobacterium containing mock, *Pdex:NbGLA1* or *Pdex:NbGLA1*^{mut}, with or without 30 µM dex treatment. Tissue was collected at the indicated times after dex treatment. Mock was collected 6 h after dex treatment (**A**). Wounding (W) was applied for 30 min with or without 6 h of DEX pre-treatment (**B**). Agrobacterium was infiltrated 48 h prior to other treatments. Data represents the average of three (**A**) or four (**B**) biological replicates ± SD. Letters above graphs indicate significant differences ($P < 0.05$; Student's *t*-test)

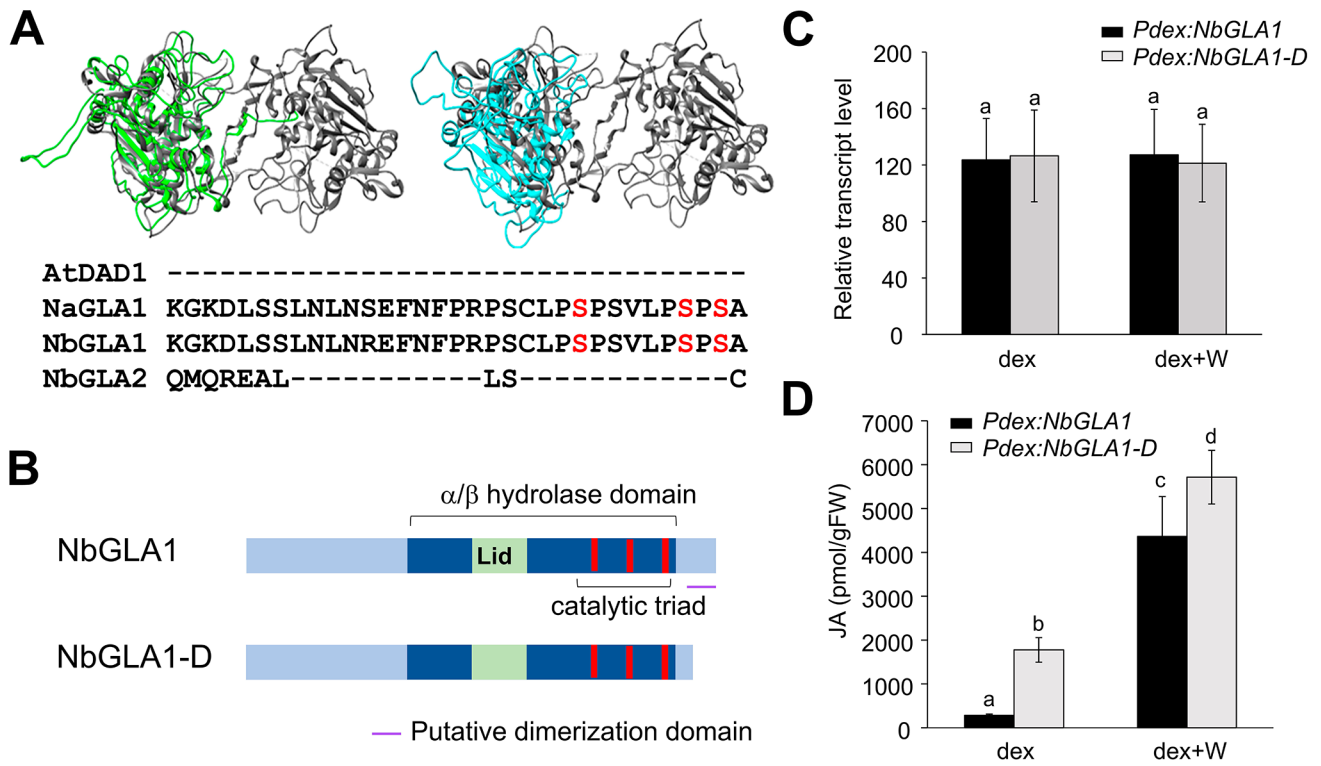

Fig. 5 Role of the C-terminal domain of NbGLA1 in wound-induced JA biosynthesis. (**A**) Homology modeling of NbGLA1 (shown in green) using the ModWeb application (see Methods). The amino acid sequence of NbGLA1 was modeled against the PDB structure 2YIJ (grey), which is a homodimer. For comparison, homology modeling of Arabidopsis AtDAD1 (cyan) is provided. Sequence alignment showing conservation of the C-terminal region between NaGLA1 and NbGLA1, but not in NbGLA2 or AtDAD1, which lack the C-terminal end. Predicted phosphorylation sites on serine (identified by MusiteDeep) are shown in red. (**B**) Schematic representation of NbGLA1 with a 33 amino acid putative C-terminal dimerization domain, which is removed in the *NbGLA1-D* construct. (**C** and **D**) RT-qPCR analysis of GLA1 transcripts (**C**) and JA (**D**) accumulation in *N. benthamiana* leaves transiently expressing the full-length (*Pdex:NbGLA1*) or truncated construct (*Pdex:NbGLA1-D*), treated with dex (30 µM, 6 h) or both dex and wounding (30 min) (dex + W) total 6 h). Relative transcript levels were normalized using *NbEF1a* as an internal reference gene and then was compared with mock-treated (infiltration solution 2 days and 0.01% (v/v) DMSO and 0.01% (v/v) Triton x-100 6 h). Letters above the graphs indicate significant differences ($P < 0.05$; Student's *t*-test). Data represent the average of three (**C**) or six (**D**) biological replicates ± SD

To assess the functional significance of this C-terminal domain, a truncated version of NbGLA1 with its 42 amino acid C-terminal segment removed was cloned into the dex-inducible vector (*Pdex:NbGLA1-D*) (Fig. 5B). Similar to the previous experiment (Fig. 4B), *N. benthamiana* leaves were infiltrated with each of the full length and truncated constructs, followed by treatment with 30 µM dex, with or without wounding, and were subjected to RNA and JA analysis (Fig. 5C and D). Both constructs were expressed to a similar extent after 6 h of dex treatment with no apparent additive effect from wounding (Fig. 5C). In the samples treated with dex-only (without wounding), the truncated *Pdex:NbGLA1-D* construct resulted in significantly higher levels of JA (approximately 1,500 pmol/gFW) compared to the full-length construct (Fig. 5D). Consistent with previous findings (Fig. 4B) (Kimberlin et al. 2022), the co-treatment of dex and wounding in the leaves infiltrated with the full-length NbGLA1 construct boosted JA accumulation (Fig. 5D). The similar treatment with the truncated construct (*Pdex:NbGLA1-D*) led to more increase in JA levels comparable to those induced by the full-length construct although the difference between the two constructs was not as great as that in the dex-only treatment (Fig. 5D). Similar results were obtained from an independent experiment (Supplemental Fig. S4). Overall, these results suggest that the removal of the 42-amino acid C-terminal domain has some influence on the ability of NbGLA1 to initiate JA biosynthesis in the absence of wounding but has a relatively less impact on its ability to boost he JA biosynthesis upon wounding.

Discussion

The initial lag period of approximately 10 min observed during the time course of JA synthesis in *N. benthamiana* (Fig. 1A and D) raised questions about the potential differences in the initiation mechanism of JA biosynthesis compared to previous reports in Arabidopsis (Kimberlin et al. 2022; Koo et al. 2009; Chung et al. 2008; Glauser et al. 2008), where increases without any delay have been observed. However, the immediate increase of OPDA upon wounding (Fig. 1B) demonstrated that the rapid initiation feature of the early steps of jasmonate biosynthesis occurring in the chloroplast is conserved in *N. benthamiana*. The pretreatment with COR, which induces the transcription of most JA biosynthetic enzymes (Attaran et al. 2014), failed to alleviate the initial lag in JA accumulation (Fig. 1D). This suggests that the expression of biosynthetic genes downstream of OPDA is unlikely to be the primary reason for the initial lag in JA production. However, the COR-pretreatment did enhance the overall levels of wound-induced JA at the peak of its accumulation (Fig. 1D). This differs from a similar experiment in Arabidopsis (Kimberlin et al. 2022) where no additive effects on wound-induced JA levels by COR were observed. The exact reason for this difference is unclear but may represent some limiting biosynthetic component(s) in *N. benthamiana* that can be derepressed by COR.

The efficient conversion of exogenously applied α-LA to OPDA and JA by *N. benthamiana* leaf discs without wounding (Fig. 1E-F) indicated that: (i) the biosynthesis of JA in *N. benthamiana* is limited by substrate availability, as reported in other species (Kimberlin et al. 2022; Vick and Zimmerman 1983; Christeller and Galis 2014; Miersch and Wasternack 2000); (ii) enzymes involved in the entire JA biosynthetic pathway are present and active in unstressed leaves; and (iii) the hydrolysis of the α-LA precursor from the membrane lipids is the most likely step that regulates the initiation of JA biosynthesis upon wounding.

Among the four NbGLAs that clustered most closely to the published NaGLA1 (Kallenbach et al. 2010) in the phylogeny, NbGLA1 exhibited the highest sequence identity at the amino acid level (> 96%) to NaGLA1. NbGLA2 closely followed next in sequence similarity (88%), but mRNA transcript analyses (Fig. 2E) revealed that *NbGLA2* is expressed weakly compared to *NbGLA1*. The induction of *NbGLA1* transcripts by wounding also differed from *NaGLA1*, whose transcripts were reported to decrease after wounding (Kallenbach et al. 2010). However, transcripts of several plastidial phospholipases were found to be induced by wounding in Arabidopsis (Kimberlin et al. 2022; Rudus et al. 2014). Gene silencing experiments using VIGS demonstrated that NbGLA1, NbGLA2, or both are the functional homologs of NaGLA1, responsible for the majority of wound-elicited JA biosynthesis in *N. benthamiana* leaves (Fig. 3C). Additional VIGS experiments specifically targeting each gene are required to determine whether one or both are involved in wound-induced JA biosynthesis.

The hypothesis that lipases must be regulated by post-translational mechanisms is based on anecdotal evidence from several seemingly paradoxical observations. It has been observed that JA biosynthesis starts rapidly upon wounding and does not require any additional gene transcription or translation (Kimberlin et al. 2022), suggesting that the lipase must pre-exist in untreated plants. However, there is little basal level of JA in leaves without injuries (Glauser et al. 2009; Koo et al. 2009; Chung et al. 2008), implying that the pre-existing lipases are quiescent. Consistent with this hypothesis, inducing *NbGLA1* expression solely through dex treatment did not result in significant JA accumulation in *N. benthamiana* leaves (Fig. 4). Similar results have been obtained from Arabidopsis, although the ability of AtDAD1 to induce JA biosynthesis without wounding varied depending on developmental stages (Kimberlin et al. 2022). Previous reports from other research groups expressing *PLA1s* under a constitutive promoter also failed to show constitutive accumulation of JA, although these plants did accumulate more JA when additionally wounded (Rudus et al. 2014; Ellinger et al. 2010). Similarly, when the dex-induced plants were further stimulated with wounding, JA synthesis increased several folds compared to wounding or dex treatment alone (Fig. 4B). This synergy cannot be explained by a simple addition of wound-induced and dex-induced JAs. In Arabidopsis, it has been demonstrated that the synergistic effect of induced lipase and wounding for JA biosynthesis can also be replicated in remote undamaged leaves through a systemic wound signal (Kimberlin et al. 2022; Koo and Howe 2009; Toyota et al. 2018). This finding suggests that the boost effect is unlikely to result from artifactual conditions caused by severe cell damage in the wounded cells. Additionally, while improbable, we cannot entirely rule out the possibility of the induced recombinant lipases enhancing other lipase activities.

The mechanism underlying this lipase activation by wounding remains unknown. Changes occurring to membrane lipid phases have been proposed to play a role in spontaneous JA synthesis (Yu et al. 2020). Two DAD1-like lipases (DALL2 and DALL3) (Supplemental Fig. S1) were reported to involve in rapid systemic JA biosynthesis in primary vascular tissues in response to wound-activated electrical signals (Morin et al. 2023). To begin investigating the underlying mechanisms of lipase regulation, we examined the NbGLA1 sequence and predicted its protein structure through homology modeling. The 33-amino acid C-terminal end of NbGLA1 emerged as a potential site for

protein-protein interaction and/or protein phosphorylation. Truncating this domain (NbGLA1-D) did not result in significant changes in wound-activated JA accumulation (cotreatment with dex and wound). However, it led to substantial increases in JA when induced by dex alone (Fig. 5D). In contrast, induction of full-length NbGLA1 by dex alone did not lead to JA increases without wounding. This indicates that the C-terminal domain may be involved in negative regulation, restricting lipase activation in the absence of wounding. However, these results are still preliminary and additional studies are needed to confirm the potential regulatory role of C-terminal domains. Specifically, it has yet to be established whether certain serine residues, which are notably abundant in this C-terminal region, are indeed subject to posttranslational protein modification, and/or whether they play a role in protein-protein interactions for the regulation of NbGLA1 activity. The ability to introduce site-directed mutations into the NbGLA1 sequence, along with the relative ease of achieving transient expression in *N. benthamiana* leaves, will be invaluable for investigating the mechanism that initiates JA biosynthesis.

Supplementary Information The online version contains supplementary material available at https://doi.org/10.1007/s11103-023-01408-7.

Acknowledgements We acknowledge Dr. Athen Kimberlin for his valuable technical assistance and helpful discussions. We thank Dr. Gary Stacey at the University of Missouri for sharing *N. benthamiana* seeds. MU Small Molecules MS Laboratory is acknowledged for their instrumental assistance with UPLC-MS/MS.

Author contributions A.J.K. conceived the original research plans. A.J.K. and R.H. designed experiments. R.H. and S.M. performed the experiments. All contributed to analyzing the data. A.J.K. and R.H. wrote the article with contributions by S.M.

Funding This work was made possible by the generous support from the National Science Foundation (grants no. IOS-1557439, IOS-1829365, and IOS-2101975), the Hatch Multi-State Research program of the National Institute of Food and Agriculture (project accession no. 1010448), and the Food for the 21st Century Program at the University of Missouri awarded to A.J.K.

Data availability All data associated with this study are described and included in this published manuscript and its supplementary information file.

Declarations

Competing interests The authors declare no competing interests.

References

Almagro Armenteros JJ, Salvatore M, Emanuelsson O, Winther O, von Heijne G, Elofsson A, Nielsen H (2019) Detecting sequence signals in targeting peptides using deep learning. Life Sci Alliance 2(5). https://doi.org/10.26508/lsa.201900429

Aoyama T, Chua NH (1997) A glucocorticoid-mediated transcriptional induction system in transgenic plants. Plant J 11(3):605–612

Attaran E, Major IT, Cruz JA, Rosa BA, Koo AJ, Chen J, Kramer DM, He SY, Howe GA (2014) Temporal dynamics of growth and photosynthesis suppression in response to jasmonate signaling. Plant Physiol 165(3):1302–1314. https://doi.org/10.1104/pp.114.239004

Bombarely A, Rosli HG, Vrebalov J, Moffett P, Mueller LA, Martin GB (2012) A draft genome sequence of Nicotiana benthamiana to enhance molecular plant-microbe biology research. Mol Plant Microbe Interact 25(12):1523–1530. https://doi.org/10.1094/mpmi-06-12-0148-ta

Burch-Smith TM, Schiff M, Liu Y, Dinesh-Kumar SP (2006) Efficient Virus-Induced Gene silencing in Arabidopsis. Plant Physiol 142(1):21–27. https://doi.org/10.1104/pp.106.084624

Christeller JT, Galis I (2014) Alpha-linolenic acid concentration and not wounding per se is the key regulator of octadecanoid (oxylipin) pathway activity in rice (Oryza sativa L.) leaves. Plant Physiol Biochem 83:117–125

Chung HS, Koo AJ, Gao X, Jayanty S, Thines B, Jones AD, Howe GA (2008) Regulation and function of Arabidopsis JASMONATE ZIM-domain genes in response to wounding and herbivory. Plant Physiol 146(3):952–964

Di Tommaso P, Moretti S, Xenarios I, Orobitg M, Montanyola A, Chang J-M, Taly J-F, Notredame C (2011) T-Coffee: a web server for the multiple sequence alignment of protein and RNA sequences using structural information and homology extension. Nucleic Acids Res 39(suppl2):W13–W17. https://doi.org/10.1093/nar/gkr245

Dommes AB, Gross T, Herbert DB, Kivivirta KI, Becker A (2019) Virus-induced gene silencing: empowering genetics in non-model organisms. J Exp Bot 70(3):757–770. https://doi.org/10.1093/jxb/ery411

Ellinger D, Stingl N, Kubigsteltig II, Bals T, Juenger M, Pollmann S, Berger S, Schuenemann D, Mueller MJ (2010) DONGLE and DEFECTIVE IN ANTHER DEHISCENCE1 lipases are not essential for wound- and pathogen-induced jasmonate biosynthesis: redundant lipases contribute to jasmonate formation. Plant Physiol 153(1):114–127

Eswar N, Webb B, Marti-Renom MA, Madhusudhan MS, Eramian D, Shen MY, Pieper U, Sali A (2006) Comparative protein structure modeling using Modeller. Curr Protoc Bioinformatics Chap 5:Unit. -5.6

Farmer EE, Ryan CA (1992) Octadecanoid precursors of jasmonic acid activate the synthesis of wound-inducible proteinase-inhibitors. Plant Cell 4(2):129–134

Fonseca S, Chini A, Hamberg M, Adie B, Porzel A, Kramell R, Miersch O, Wasternack C, Solano R (2009) (+)-7-iso-jasmonoyl-l-isoleucine is the endogenous bioactive jasmonate. Nat Chem Biol 5(5):344–350. https://doi.org/10.1038/nchembio.161

Glauser G, Grata E, Dubugnon L, Rudaz S, Farmer EE, Wolfender JL (2008) Spatial and temporal dynamics of jasmonate synthesis and accumulation in Arabidopsis in response to wounding. J Biol Chem 283(24):16400–16407

Glauser G, Dubugnon L, Mousavi SA, Rudaz S, Wolfender JL, Farmer EE (2009) Velocity estimates for signal propagation leading to systemic jasmonic acid accumulation in wounded Arabidopsis. J Biol Chem 284(50):34506–34513

Howe GA, Major IT, Koo AJ (2018) Modularity in jasmonate signaling for multistress resilience. Annu Rev Plant Biol 69:387–415. https://doi.org/10.1146/annurev-arplant-042817-040047

Hyun Y, Choi S, Hwang HJ, Yu J, Nam SJ, Ko J, Park JY, Seo YS, Kim EY, Ryu SB, Kim WT, Lee YH, Kang H, Lee I (2008) Cooperation and functional diversification of two closely related galactolipase genes for jasmonate biosynthesis. Dev Cell 14(2):183–192

Ishiguro S, Kawai-Oda A, Ueda J, Nishida I, Okada K (2001) The DEFECTIVE IN ANTHER DEHISCIENCE gene encodes a novel phospholipase A1 catalyzing the initial step of jasmonic acid biosynthesis, which synchronizes pollen maturation, anther dehiscence, and flower opening in Arabidopsis. Plant Cell 13(10):2191–2209

Kallenbach M, Alagna F, Baldwin IT, Bonaventure G (2010) Nicotiana attenuata SIPK, WIPK, NPR1, and fatty acid-amino acid conjugates participate in the induction of jasmonic acid biosynthesis by affecting early enzymatic steps in the pathway. Plant Physiol 152(1):96–106

Katsir L, Chung HS, Koo AJ, Howe GA (2008a) Jasmonate signaling: a conserved mechanism of hormone sensing. Curr Opin Plant Biol 11(4):428–435. https://doi.org/10.1016/j.pbi.2008.05.004

Katsir L, Schilmiller AL, Staswick PE, He SY, Howe GA (2008b) COI1 is a critical component of a receptor for jasmonate and the bacterial virulence factor coronatine. Proc Natl Acad Sci U S A 105(19):7100–7105

Kelly AA, Feussner I (2016) Oil is on the agenda: lipid turnover in higher plants. Biochim Biophys Acta 4(16):30117–30112

Kimberlin AN, Holtsclaw RE, Zhang T, Mulaudzi T, Koo AJ (2022) On the initiation of jasmonate biosynthesis in wounded leaves. Plant Physiol 189(4):1925–1942. https://doi.org/10.1093/plphys/kiac163

Koch T, Krumm T, Jung V, Engelberth J, Boland W (1999) Differential induction of plant volatile biosynthesis in the lima bean by early and late intermediates of the octadecanoid-signaling pathway. Plant Physiol 121(1):153–162

Koo AJ (2018) Metabolism of the plant hormone jasmonate: a sentinel for tissue damage and master regulator of stress response. Phytochem Rev 17(1):51–80. https://doi.org/10.1007/s11101-017-9510-8

Koo AJ, Howe GA (2009) The wound hormone jasmonate. Phytochemistry 70(13–14):1571–1580. https://doi.org/10.1016/j.phytochem.2009.07.018

Koo AJ, Gao X, Jones AD, Howe GA (2009) A rapid wound signal activates the systemic synthesis of bioactive jasmonates in Arabidopsis. Plant J 59(6):974–986. https://doi.org/10.1111/j.1365-313X.2009.03924.x

Koo AJ, Thireault C, Zemelis S, Poudel AN, Zhang T, Kitaoka N, Brandizzi F, Matsuura H, Howe GA (2014) Endoplasmic reticulum-associated inactivation of the hormone jasmonoyl-L-isoleucine by multiple members of the cytochrome P450 94 family in Arabidopsis. J Biol Chem 289(43):29728–29738. https://doi.org/10.1074/jbc.M114.603084

Kumar S, Stecher G, Li M, Knyaz C, Tamura K (2018) MEGA X: Molecular Evolutionary Genetics Analysis across Computing platforms. Mol Biol Evol 35(6):1547–1549. https://doi.org/10.1093/molbev/msy096

Letunic I, Bork P (2021) Interactive tree of life (iTOL) v5: an online tool for phylogenetic tree display and annotation. Nucleic Acids Res 49(W1):W293–W296. https://doi.org/10.1093/nar/gkab301

McConn M, Browse J (1996) The critical requirement for linolenic acid is pollen development, not photosynthesis, in an Arabidopsis mutant. Plant Cell 8(3):403–416

Mielke S, Zimmer M, Meena MK, Dreos R, Stellmach H, Hause B, Voiniciuc C, Gasperini D (2021) Jasmonate biosynthesis arising from altered cell walls is prompted by turgor-driven mechanical compression. Sci Adv 7(7). https://doi.org/10.1126/sciadv.abf0356

Miersch O, Wasternack C (2000) Octadecanoid and jasmonate signaling in tomato (Lycopersicon esculentum Mill.) Leaves: endogenous jasmonates do not induce jasmonate biosynthesis. Biol Chem 381(8):715–722

Morin H, Chételat A, Stolz S, Marcourt L, Glauser G, Wolfender JL, Farmer EE (2023) Wound-response jasmonate dynamics in the primary vasculature. New Phytol 240(4):1484–1496. https://doi.org/10.1111/nph.19207

Pieper U, Eswar N, Webb BM, Eramian D, Kelly L, Barkan DT, Carter H, Mankoo P, Karchin R, Marti-Renom MA, Davis FP, Sali A (2009) MODBASE, a database of annotated comparative protein structure models and associated resources. Nucleic Acids Res 37(Database issue):D347–354. https://doi.org/10.1093/nar/gkn791

Pluskota WE, Qu N, Maitrejean M, Boland W, Baldwin IT (2007) Jasmonates and its mimics differentially elicit systemic defence responses in Nicotiana attenuata. J Exp Bot 58(15–16):4071–4082

Rudus I, Terai H, Shimizu T, Kojima H, Hattori K, Nishimori Y, Tsukagoshi H, Kamiya Y, Seo M, Nakamura K, Kepczynski J, Ishiguro S (2014) Wound-induced expression of DEFECTIVE IN ANTHER DEHISCENCE1 and DAD1-like lipase genes is mediated by both CORONATINE INSENSITIVE1-dependent and independent pathways in Arabidopsis thaliana. Plant Cell Rep 33(6):849–860

Ryu SB (2004) Phospholipid-derived signaling mediated by phospholipase A in plants. Trends Plant Sci 9(5):229–235

Ryu CM, Anand A, Kang L, Mysore KS (2004) Agrodrench: a novel and effective agroinoculation method for virus-induced gene silencing in roots and diverse solanaceous species. Plant J 40(2):322–331. https://doi.org/10.1111/j.1365-313X.2004.02211.x

Schaller A, Stintzi A (2009) Enzymes in jasmonate biosynthesis - structure, function, regulation. Phytochemistry 70(13–14):1532–1538

Scholz SS, Reichelt M, Boland W, Mithofer A (2015) Additional evidence against jasmonate-induced jasmonate induction hypothesis. Plant Sci 239:9–14. https://doi.org/10.1016/j.plantsci.2015.06.024

Staswick PE, Tiryaki I (2004) The oxylipin signal jasmonic acid is activated by an enzyme that conjugates it to isoleucine in Arabidopsis. Plant Cell 16(8):2117–2127

Toyota M, Spencer D, Sawai-Toyota S, Jiaqi W, Zhang T, Koo AJ, Howe GA, Gilroy S (2018) Glutamate triggers long-distance, calcium-based plant defense signaling. Science 361(6407):1112–1115. https://doi.org/10.1126/science.aat7744

Vick BA, Zimmerman DC (1983) The biosynthesis of jasmonic acid: a physiological role for plant lipoxygenase. Biochem Biophys Res Commun 111(2):470–477

Wang X (2001) Plant phospholipases. Annu Rev Plant Physiol Plant Mol Biol 52:211–231

Wang K, Guo Q, Froehlich JE, Hersh HL, Zienkiewicz A, Howe GA, Benning C (2018) Two abscisic acid-responsive plastid lipase genes involved in jasmonic acid biosynthesis in Arabidopsis thaliana. Plant Cell 30(5):1006–1022. https://doi.org/10.1105/tpc.18.00250

Wang D, Liu D, Yuchi J, He F, Jiang Y, Cai S, Li J, Xu D (2020) MusiteDeep: a deep-learning based webserver for protein post-translational modification site prediction and visualization. Nucleic Acids Res 48(W1):W140–w146. https://doi.org/10.1093/nar/gkaa275

Wasternack C (2007) Jasmonates: an update on biosynthesis, signal transduction and action in plant stress response, growth and development. Ann Bot (Lond) 100:681–697

Wasternack C, Feussner I (2018) The oxylipin pathways: biochemistry and function. Annu Rev Plant Biol 69:363–386. https://doi.org/10.1146/annurev-arplant-042817-040440

Wasternack C, Hause B (2013) Jasmonates: biosynthesis, perception, signal transduction and action in plant stress response, growth and development. An update to the 2007 review in annals of Botany. Ann Bot 111(6):1021–1058

Yang W, Devaiah SP, Pan X, Isaac G, Welti R, Wang X (2007) AtPLAI is an acyl hydrolase involved in basal jasmonic acid production and Arabidopsis tesistance to Botrytis Cinerea. J Biol Chem 282(25):18116–18128. https://doi.org/10.1074/jbc.M700405200

Yang J, Yan R, Roy A, Xu D, Poisson J, Zhang Y (2015) The I-TASSER suite: protein structure and function prediction. Nat Methods 12(1):7–8. https://doi.org/10.1038/nmeth.3213

Yu CW, Lin YT, Li HM (2020) Increased ratio of galactolipid MGDG: DGDG induces jasmonic acid overproduction and changes chloroplast shape. New Phytol. https://doi.org/10.1111/nph.16766